Effects of Subcarrier Power Allocation on an Interference Avoidance Code Assignment Strategy for Multirate MC-DS-CDMA Systems

Chih-Wen Chang, *Member, IEEE*, and Li-Chun Wang, *Senior Member, IEEE*

***Abstract*—In this paper, we propose a joint subcarrier power allocation (SPA) and code assignment scheme for the synchronous multirate multicarrier direct-sequence code-division multiple-access (MC-DS-CDMA) system with time- and frequency-domain spreadings. Based on the newly defined metric multiple-access interference (MAI) coefficient, the proposed code assignment strategy can quantitatively predict the incurred MAI before assigning a spreading code. The SPA mechanism aims to maximize the received signal power. In addition to lowering the MAI, the proposed code assignment strategy further considers the compactness of the assigned codes in the entire 2-D tree structure. The simulation results show that the proposed joint SPA and code assignment strategy not only can reach a better received signal quality but can also achieve a high call admission rate.**

***Index Terms*—Code assignment, interference avoidance, multicarrier direct-sequence code-division multiple access (MC-DS-CDMA), multiple-access interference (MAI) coefficient, subcarrier power allocation (SPA).**

I. Introduction

COMBINING the advantages of orthogonal frequency-division multiplexing (OFDM) and spreading spectrum systems, multicarrier code-division multiple access (MC-CDMA) has the potential to be a strong candidate for future broadband wireless communication systems [1]–[3]. The advantages of the MC-CDMA system include the robustness against the frequency-selective fading channel, the flexibility in system design, and the low detection complexity [4]–[7]. Generally, MC-CDMA can be divided into the following three categories: 1) MC-CDMA with pure frequency spreading; 2) multicarrier direct-sequence CDMA (MC-DS-CDMA) with pure time spreading; and 3) MC-DS-CDMA with joint time and frequency spreading [(TF)-domain spreading]. By adjusting spreading gains in both the time and frequency domains, the MC-DS-CDMA with TF-domain spreading can outperform the other two MC-CDMA schemes in supporting versatile multirate services in diverse environments [8]–[12].

Furthermore, subcarrier power is another degree of freedom for the MC-DS-CDMA system. However, it is challenging to allocate subcarrier power in a multiuser environment. An optimal power allocation scheme with a maximized received signal power for a particular user may also produce excessive interference to other users, which may also lower the call admission rate. Thus, we are motivated to propose a joint subcarrier power allocation (SPA) and code assignment aimed at maximizing the signal power through SPA while eliminating multiple-access interference (MAI) through a novel code assignment scheme. To achieve this goal, we first maximize the signal quality by allocating subcarrier power. On top of this allocated subcarrier power, we develop a code assignment strategy to maintain high call admission rates with less MAI. We define a new performance metric called the MAI coefficient. Through the bit-error-rate (BER) analysis associated with the SPA mechanism, we show that the MAI coefficient can quantitatively predict the incurred MAI before assigning a spreading code. Thus, with the help of the MAI coefficient, an interference avoidance code assignment can be designed to choose a code with the minimum incurred MAI. The simulation results show that the proposed joint SPA and interference avoidance code assignment strategy can significantly improve the received signal quality. Furthermore, the code assignment considers the 2-D code tree structure in assigning a code to a user. Thus, the code assignment can also maintain good call admission rates.

In the literature, the SPA mechanism, MAI elimination, and code assignment associated with the code tree structure are not jointly considered in the MC-DS-CDMA systems. From the aspect of SPA, some SPA mechanisms aimed at improving BER performance have been proposed [13], [14]. In [13], the SPA mechanism was considered in a nonspread spectrum multicarrier system. In [14], Long and Chew proposed an adaptive subcarrier allocation policy for the frequency-hopping MC-DS-CDMA systems to avoid collision between users when loading bits to subcarriers. From the aspect of MAI elimination, the interference rejection and interference-free spreading codes were proposed for the asynchronous MC-DS-CDMA in [15] and [16], respectively. In [17], an MAI-minimized signature waveform was proposed to minimize MAI for MC-DS-CDMA systems. From the code assignment aspect, Amadei *et al.* [18] and Manzoli and Merani [19] proposed a code assignment strategy based on dual quasi-orthogonal and Walsh codes to

Manuscript received June 7, 2007; revised March 16, 2007 and July 25, 2007. This work was supported by the National Science Council, Taiwan, under Contract 94-2213-E-009-060, Contract 95-2218-E-006-041, and Contract 96-2221-E-006-020. The review of this paper was coordinated by Dr. K. Molnar.

C.-W. Chang is with the Institute of Computer and Communication Engineering, National Cheng Kung University, Tainan 701, Taiwan, R.O.C. (e-mail: cwchang@ee.ncku.edu.tw).

L.-C. Wang is with the Department of Communication Engineering, National Chiao Tung University, Hsinchu 300, Taiwan, R.O.C. (e-mail: lichun@cc.nctu.edu.tw).

Color versions of one or more of the figures in this paper are available online at http://ieeexplore.ieee.org.

Digital Object Identifier 10.1109/TVT.2007.909300

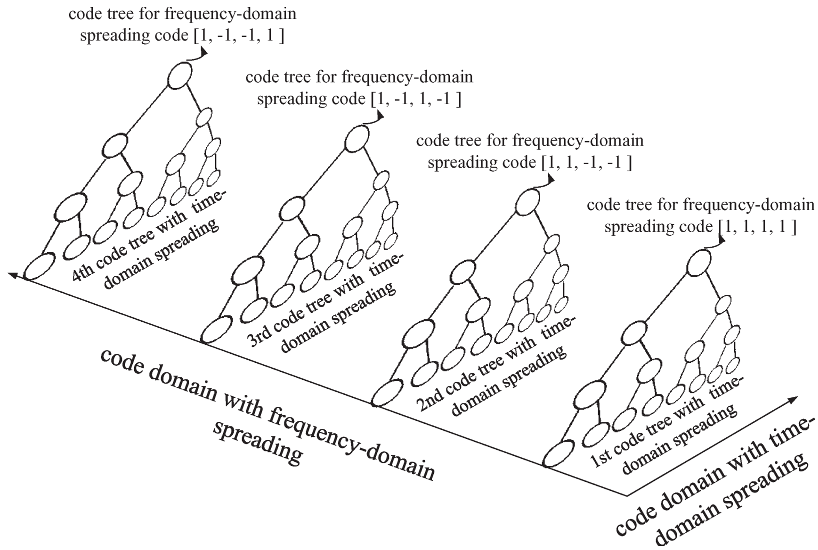

Fig. 1. Two-dimensional OVSF code tree when the frequency-domain spreading factor is 4.

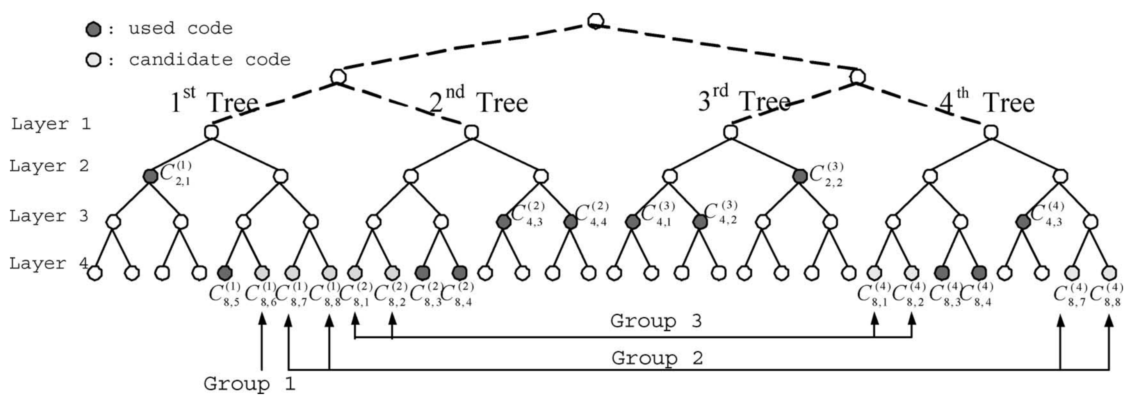

Fig. 2. Example of allocating a code with frequency-domain spreading factor $M = 4$ and time-domain spreading factor $SF = 8$ in the 2-D code tree.

reduce MAI in MC-DS-CDMA systems. However, in the above MC-DS-CDMA systems [14]–[19], all belong to the MC-DS-CDMA with 1-D time-domain spreading. For the MC-DS-CDMA system with TF-domain spreading, Yang *et al.* [10] proposed novel 2-D orthogonal variable-spreading factor (OVSF) codes but ignored the impact of frequency-selective diversity. Furthermore, the MAI rejection property of [10] may disappear because the zero autocorrelation sidelobes and the zero cross-correlation functions are no longer true when the subcarriers carrying the same data bit experience independent fading. In our previous paper [20], we proposed a novel interference avoidance code assignment strategy without taking the SPA mechanism into consideration.

In this paper, we investigate the MAI impact caused by reusing time-domain spreading codes in the MC-DS-CDMA, which is not considered in [13]–[19]. Specifically, we consider the joint impact of MAI and the compactness of the code tree structure, as well as the SPA mechanism. Moreover, we consider a downlink MC-DS-CDMA system with a constant frequency diversity gain. The rest of this paper is organized as follows. The 2-D OVSF code tree structure and the signal model in the MC-DS-CDMA system with TF-domain spreading are introduced in Section II. In Sections III and IV, we propose the SPA mechanism and define the performance metric MAI coefficient, respectively. Section V presents a joint SPA and interference avoidance code assignment strategy for the multirate MC-DS-CDMA system with TF-domain spreading. Simulation results are provided in Section VI. We give our concluding remarks in Section VII.

II. SYSTEM MODEL

A. Background

To spread in both the time and frequency domains, the OVSF code tree in a multirate MC-DS-CDMA system has a 2-D structure, as shown in Fig. 1. In the figure, the total spreading factor is $SF_f \times SF_t$, where the frequency-domain spreading factor $SF_f = 4$ and the time-domain spreading factor $SF_t = 1 \sim 8$, respectively. As shown in the figure, each branch of the code tree in the time-domain spreading is associated with a frequency-domain spreading code. For ease

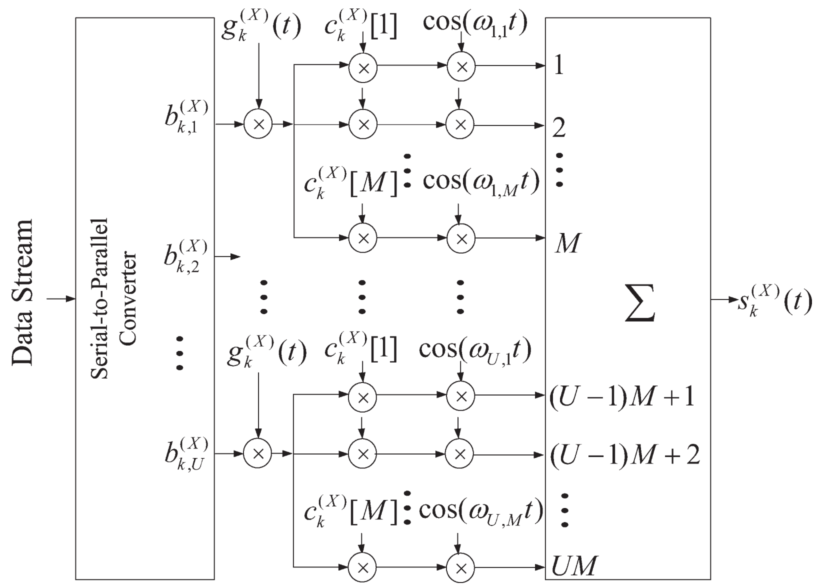

Fig. 3. Transmitter structure of the MC-DS-CDMA using TF-domain spreading codes.

of illustration, we spread the 2-D code tree in Fig. 1 onto a plane as in Fig. 2, where "●" and "●" stand for the "used code" and "candidate code" for a requested code of $SF_t = 8$, respectively. The orthogonality between any two codes can be maintained if they do not have an ancestor–descendant relationship. However, due to frequency-selective fading, the orthogonality of the OVSF codes positioned in the different branches of the 2-D code tree may not be satisfied. Two codes in the 2-D OVSF code tree are called *related codes* if they have an ancestor–descendant relationship in the time-domain spreading, such as $C_{4,2}^{(3)} = [1 \quad 1 \quad -1 \quad -1]$ and $C_{8,3}^{(2)} = [1 \quad 1 \quad -1 \quad -1 \quad 1 \quad 1 \quad -1 \quad -1]$. Note that in a frequency-selective fading channel, the orthogonality of the two related codes $C_{4,2}^{(3)}$ and $C_{8,3}^{(2)}$ are not guaranteed. For a clear illustration of the related codes, see the grid representation of the 2-D code tree for the MC-DS-CDMA systems in [20].

B. Transmitted Signal

The transmitter structure in the MC-DS-CDMA system with TF-domain spreading is shown in Fig. 3. A serial-to-parallel converter is applied to reduce the subcarrier data rate by converting data streams with bit duration $T_{b,k}^{(\mathbf{X})}$ into U reduced-rate parallel substreams with new bit duration $T_k^{(\mathbf{X})} = UT_{b,k}^{(\mathbf{X})}$ for user k in group $\mathbf{X} \in \{\mathbf{A}, \mathbf{B}, \mathbf{C}\}$. Each substream experiences a frequency-flat (or nondispersive) fading. Then, for each substream, a spreading code $g_k^{(\mathbf{X})}(t)$ is used to spread data signals in the time domain. After being copied to M subcarriers, the data in each substream is multiplied by a frequency-domain spreading code $\{c_k^{(\mathbf{X})}[j]\}$. In this case, the frequency-domain spreading gain is M. The user group $\mathbf{X}$ is defined as follows. Let $g_o(t)$ and $c_o[j]$ be the time-domain spreading code and the frequency-domain spreading code of the reference user, respectively. Then, similar to [9] and [12], the interfering users in the MC-DS-CDMA system can be categorized into the following three groups:

$$(1)\ \text{group } \mathbf{A}: \begin{cases} \dfrac{1}{T_o}\displaystyle\int_0^{T_o} g_k^{(\mathbf{A})}(t) g_o(t)dt \neq 0 \\ \dfrac{1}{M}\displaystyle\sum_{j=1}^{M} c_k^{(\mathbf{A})}[j] c_o[j] = 0 \end{cases}$$

$$(2)\ \text{group } \mathbf{B}: \begin{cases} \dfrac{1}{T_o}\displaystyle\int_0^{T_o} g_k^{(\mathbf{B})}(t) g_o(t)dt = 0 \\ \dfrac{1}{M}\displaystyle\sum_{j=1}^{M} c_k^{(\mathbf{B})}[j] c_o[j] \neq 0 \end{cases}$$

$$(3)\ \text{group } \mathbf{C}: \begin{cases} \dfrac{1}{T_o}\displaystyle\int_0^{T_o} g_k^{(\mathbf{C})}(t) g_o(t)dt = 0 \\ \dfrac{1}{M}\displaystyle\sum_{j=1}^{M} c_k^{(\mathbf{C})}[j] c_o[j] = 0. \end{cases}$$

The transmitted signal of user k in group $\mathbf{X} \in \{\mathbf{A}, \mathbf{B}, \mathbf{C}\}$ can be expressed as

$$s_k^{(\mathbf{X})}(t) = \sum_{i=1}^{U}\sum_{j=1}^{M} \sqrt{2P_{k,i,j}^{(\mathbf{X})}} b_{k,i}^{(\mathbf{X})}(t) g_k^{(\mathbf{X})}(t) c_k^{(\mathbf{X})}[j] \times \cos\left(2\pi f_{i,j} t + \varphi_{k,i,j}^{(\mathbf{X})}\right) \quad (1)$$

where $P_{k,i,j}^{(\mathbf{X})}$, $\{f_{i,j}\}$, and $\{\varphi_{k,i,j}^{(\mathbf{X})}\}$ represent the transmitted power, the jth subcarrier frequency, and the initial phase in the ith substream, respectively. The waveform of the ith

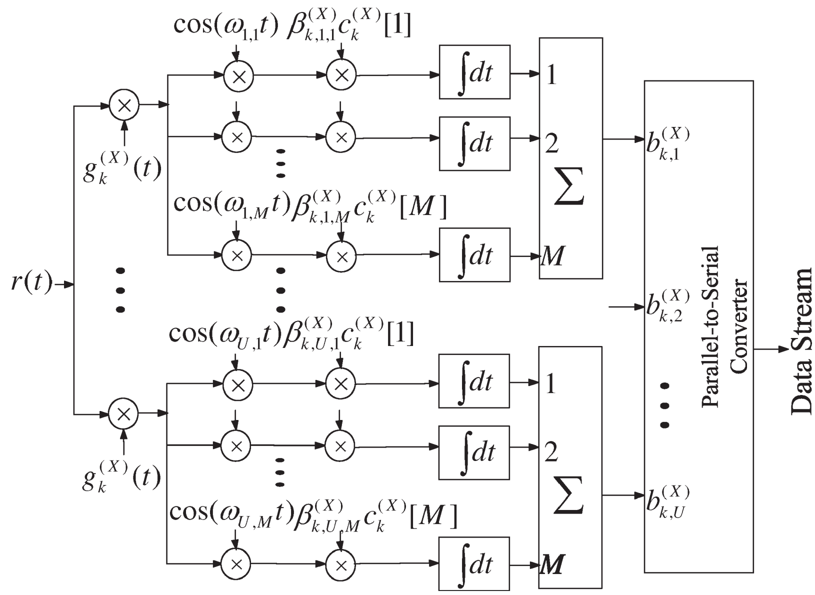

Fig. 4. Receiver structure of the MC-DS-CDMA using TF-domain spreading codes.

substream $b^{(\mathbf{X})}_{k,i}(t) = \sum_{h=-\infty}^{\infty} b^{(\mathbf{X})}_{k,i}[h] P_{T^{(\mathbf{X})}_k}(t - hT^{(\mathbf{X})}_k)$ contains rectangular pulses of duration $T^{(\mathbf{X})}_k$, where $b^{(\mathbf{X})}_{k,i}[h] = \pm 1$ with equal probability. The time-domain spreading code $g^{(\mathbf{X})}_k(t) = \sum_{\ell=-\infty}^{\infty} g^{(\mathbf{X})}_k[\ell] P_{T_c}(t - \ell T_c)$ represents the chip sequence of the rectangular pulses of duration T_c, where $g^{(\mathbf{X})}_k[\ell] = \pm 1$ with equal probability. Note that the time-domain spreading factor of user k in group $\mathbf{X}$ is $G^{(\mathbf{X})}_k = T^{(\mathbf{X})}_k / T_c$.

C. Received Signal

The receiver structure of the MC-DS-CDMA using TF-domain spreading codes is shown in Fig. 4. Recall that each substream experiences flat Rayleigh fading. Then, the received signal of the reference user (denoted by r_o) in the synchronous transmission can be expressed as

$$\begin{aligned} r_o(t) &= \sum_{i=1}^{U}\sum_{j=1}^{M} \sqrt{2P_{o,i,j}}\,\alpha_{o,i,j} b_{o,i}(t) g_o(t) c_o[j] \\ &\quad \times \cos(2\pi f_{i,j} t + \phi_{i,j}) \\ &\quad + \sum_{\mathbf{X}\in\{\mathbf{A},\mathbf{B},\mathbf{C}\}} \sum_{k=1}^{K_{\mathbf{X}}} \sum_{i=1}^{U}\sum_{j=1}^{M} \sqrt{2P^{(\mathbf{X})}_{k,i,j}}\,\alpha_{o,i,j} b^{(\mathbf{X})}_{k,i}(t) \\ &\quad \times g^{(\mathbf{X})}_k(t) c^{(\mathbf{X})}_k[j] \cos(2\pi f_{i,j} t + \phi_{i,j}) + n(t) \end{aligned} \tag{2}$$

where $P_{o,i,j}$ and $\alpha_{o,i,j}$ are the reference user's transmission power and the channel amplitude for the jth subcarrier of the ith substream, $K_{\mathbf{X}}$ is the number of users in the group $\mathbf{X}$, and $n(t)$ is the white Gaussian noise with a double-sided power spectrum density of $N_0/2$. In (2), $\phi_{i,j} = \varphi_{i,j} + \psi_{i,j}$ is uniformly distributed in $[0, 2\pi)$, where $\varphi_{i,j}$ is the initial phase of the reference user, and $\psi_{i,j}$ is the channel's phase of the jth subcarrier in the ith substream.

Without loss of generality, let the bit of interest be $b_{o,s}[0]$, denoting the first bit in the sth substream from the reference user. After time-domain despreading, the output signal for the reference user in the vth subcarrier of the sth substream can be expressed as

$$\begin{aligned} Y_{o,s,v} &= \int_0^{T_o} r_o(t)\beta_{o,s,v} g_o(t) c_o[v] \cos(2\pi f_{s,v} t + \phi_{s,v}) dt \\ &= \frac{T_o}{\sqrt{2}} \Bigg\{ b_{o,s}[0]\sqrt{P_{o,s,v}}\,\alpha_{o,s,v}\beta_{o,s,v} \\ &\qquad + \sum_{\mathbf{X}\in\{\mathbf{A},\mathbf{B},\mathbf{C}\}} \sum_{k=1}^{K_{\mathbf{X}}} I^{(\mathbf{X})}_{k,s,v} + n_{s,v} \Bigg\} \end{aligned} \tag{3}$$

where T_o is the bit duration of the reference user, $\beta_{o,s,v}$ are the weights for a certain combining scheme, $I^{(\mathbf{X})}_{k,s,v}$ denotes the MAI induced from user k of group $\mathbf{X}$ to the vth subcarrier of the sth substream of the reference user, and $n_{s,v}$ is the white Gaussian noise with zero mean and variance of $(|\beta_{o,s,v}|^2/2)(N_o/T_0)$. The MAI terms $I^{(\mathbf{X})}_{k,s,v}$ in (3) can be expressed as

$$\begin{aligned} I^{(\mathbf{X})}_{k,s,v} &= \sqrt{P^{(\mathbf{X})}_{k,s,v}}\,\frac{\alpha_{o,s,v}\beta_{o,s,v} c^{(\mathbf{X})}_k[v] c_o[v]}{T_o} \\ &\quad \times \int_0^{T_o} b^{(\mathbf{X})}_{k,s}(t) g^{(\mathbf{X})}_k(t) g_o(t) dt. \end{aligned} \tag{4}$$

Then, combining M subcarriers, the decision variable of $b_{o,s}[0]$ for the reference user becomes

$$\begin{aligned} Y_{o,s} &= \sum_{v=1}^{M} Y_{o,s,v} \\ &= \frac{T_o}{\sqrt{2}} \left\{ \underbrace{b_{o,s}[0] \sum_{v=1}^{M} \sqrt{P_{o,s,v}} \alpha_{o,s,v} \beta_{o,s,v}}_{\text{desired signal}} \right. \\ &\qquad \left. + \underbrace{\sum_{\mathbf{X} \in \{\mathbf{A},\mathbf{B},\mathbf{C}\}} \sum_{k=1}^{K_{\mathbf{X}}} \sum_{v=1}^{\mathbf{M}} I_{k,s,v}^{(\mathbf{X})}}_{\text{MAI}} + \sum_{v=1}^{M} n_{s,v} \right\} \end{aligned} \tag{5}$$

where $Y_{o,s,v}$ is given in (3).

In (5), we face the problem of simultaneously maximizing the desired signal's power and eliminating the MAI. Note that as a user maximizes its received signal power according to a particular SPA, it may result in excessive MAI to other users. The MAI occurs when user k adjusts $P_{k,s,v}^{(\mathbf{X})}$. It is difficult to please each user just by a particular SPA mechanism. One of the goals in this paper is to find a method to improve the desired signal quality and to control MAI.

III. SPA MECHANISM

The goal of this section is to propose an SPA mechanism that will optimize the signal of the desired user in (5). The transmission power is constrained to avoid the so-called party effect in the CDMA system. The party effect is a situation where all users continuously increase transmission power, but indeed, the signal quality is not improved due to increasing interference. The transmission power constraint imposed on the reference user can be expressed as

$$\sum_{v=1}^{M} P_{o,s,v} = P_o \tag{6}$$

where P_o is assumed to be proportional to the reference user's transmission rate, as in [12], [21], and [22]. From (5), the SPA mechanism that will maximize the desired signal can be formulated as follows:

$$\begin{aligned} \text{maximize} \quad & \sum_{v=1}^{M} \sqrt{P_{o,s,v}} \alpha_{o,s,v} \beta_{o,s,v} \\ \text{subject to} \quad & \sum_{v=1}^{M} P_{o,s,v} = P_o. \end{aligned} \tag{7}$$

According to the maximal ratio combining criteria, the subcarrier's signal is maximized when $\beta_{o,s,v} = \alpha_{o,s,v}^*$, with the condition of a Gaussian-approximated MAI as in [6], [12], and [20]. By applying the Lagrange multiplier method, we can obtain the Lagrange function as

$$\begin{aligned} J(P_{o,s,1}, \ldots, P_{o,s,M}) \\ = \sum_{v=1}^{M} \sqrt{P_{o,s,v}} |\alpha_{o,s,v}|^2 + \lambda \left(\sum_{v=1}^{M} P_{o,s,v} - P_o \right) \end{aligned} \tag{8}$$

where λ is the Lagrange multiplier. Differentiating (8) with respect to $P_{o,s,v}$ and setting it to zero, it follows that

$$\frac{1}{2\sqrt{P_{o,s,v}}} |\alpha_{o,s,v}|^2 + \lambda = 0, \qquad v \in \{1, 2, \ldots, M\}. \tag{9}$$

By solving (6) and (9), we can obtain

$$P_{o,s,v} = \frac{|\alpha_{o,s,v}|^4}{\sum_{v=1}^{M} |\alpha_{o,s,v}|^4} P_o \tag{10}$$

which can maximize the desired signal in (5). Similarly, we can also have

$$P_{k,s,v}^{(\mathbf{X})} = \frac{\left|\alpha_{k,s,v}^{(\mathbf{X})}\right|^4}{\sum_{v=1}^{M} \left|\alpha_{k,s,v}^{(\mathbf{X})}\right|^4} P_k^{(\mathbf{X})} \tag{11}$$

where $\alpha_{k,s,v}^{(\mathbf{X})}$ is the channel amplitude for the sth subcarrier of the vth substream of the interfering user. Note that $P_k^{(\mathbf{X})}/P_o = R_k^{(\mathbf{X})}/R_o$, where R_o and $R_k^{(\mathbf{X})}$ are the transmission rates of the reference user and user k in group $\mathbf{X}$, respectively.

IV. MAI COEFFICIENT

In this section, we define a performance metric MAI coefficient to quantize the effect of MAI imposed on each code channel. After some derivations, we can define the received E_b/N_0 (denoted by γ), shown in (12) at the bottom of the next page, where G_0 is the time-domain spreading factor of the reference user, and R_o and $R_k^{(\mathbf{A})}$ are the transmission rates of the reference user and user, k in group $\mathbf{A}$, respectively. The detailed derivations of (12) are discussed in Appendix A. Assume that the fading parameters in the MAI term of (12) are independent because the downlink MAI resulted from the subcarriers that reused time-domain spreading codes in different frequency-domain code trees. By observing the MAI term of γ in (12), we find that the term $2P_oG_o \sum_{v=1}^{M} |\alpha_{o,s,v}|^4 \mathrm{E}[|\alpha_{k,s,v}^{(\mathbf{A})}|^4 / \sum_{i=1}^{M} |\alpha_{k,s,i}^{(\mathbf{A})}|^4]$ is common to all the $K_{\mathbf{A}}$ interfering users. As a result, we can just use $\sum_{k=1}^{K_{\mathbf{A}}} \sum_{\ell=0}^{L_k^{(\mathbf{A})}-1} R_k^{(\mathbf{A})}/[R_o(L_k^{(\mathbf{A})})^2]$ to characterize the downlink MAI in the MC-DS-CDMA system. There are two possible scenarios, as described below.

1) **MAI from high data rate users:** In this case, $R_k^{(\mathbf{A})}/R_o = T_o/T_k^{(\mathbf{A})} = L_k^{(\mathbf{A})} > 1$. Subsequently, we can obtain

$$\sum_{k=1}^{K_{\mathbf{A}}} \sum_{\ell=0}^{L_k^{(\mathbf{A})}-1} \frac{R_k^{(\mathbf{A})}}{R_o \left(L_k^{(\mathbf{A})}\right)^2} = \sum_{k=1}^{K_{\mathbf{A}}} \sum_{\ell=0}^{L_k^{(\mathbf{A})}-1} \frac{1}{L_k^{(\mathbf{A})}} = \sum_{k=1}^{K_{\mathbf{A}}} 1. \tag{13}$$

2) **MAI from low data rate users:** Let $L_k^{(\mathbf{A})} = 1$ in the MAI term of (12). Then, it follows that

$$\sum_{k=1}^{K_{\mathbf{A}}} \sum_{\ell=0}^{L_k^{(\mathbf{A})}-1} \frac{R_k^{(\mathbf{A})}}{R_o \left(L_k^{(\mathbf{A})}\right)^2} = \sum_{k=1}^{K_{\mathbf{A}}} \frac{R_k^{(\mathbf{A})}}{R_o}. \tag{14}$$

Note that $R_k^{(\mathbf{A})}/R_o < 1$ in this case.

By observing (13) and (14), we can define the downlink *MAI coefficient* in the MC-DS-CDMA system with TF-domain spreading as

$$\kappa = \sum_{k=1}^{K_{\mathbf{A}}} \mathbf{min}\left(1, \frac{R_k^{(\mathbf{A})}}{R_o}\right). \tag{15}$$

V. Joint SPA and Interference Avoidance Code Assignment Strategy

A. Principles

In this section, we propose to integrate the SPA mechanism and the interference avoidance code assignment strategy to simultaneously optimize the received signal power and eliminate the MAI. In principle, the joint scheme consists of the following two steps: 1) the SPA mechanism and 2) the code assignment, as shown in Fig. 5(a). In the first step, each user applies the SPA mechanism to greedily maximize his own received signal power. In the second step, the interference avoidance code assignment is used to pick a spreading code that produces less MAI, as shown in Fig. 5(b). Let $\{C_{SF,j}^{(i)}\}$ be the set of candidate codes with TF-domain spreading factors M and SF, respectively, where $1 \leq i \leq M$, and $1 \leq j \leq SF$. Denote $\mathbf{R_c}(C_{SF,j}^{(i)})$ as the set of codes related to $C_{SF,j}^{(i)}$. The joint SPA and code assignment strategy is summarized in the following two steps.

Step 1) Each user implements the SPA mechanism according to (10) and (11).

Step 2) With the aid of the MAI coefficient, the interference avoidance code assignment strategy has the following three stages, as shown in Fig. 5(b).

Stage 1) Estimate the incurred MAI when assigning code $C_{SF,j}^{(i)}$ by calculating the sum of the MAI coefficient increments of the codes in $\mathbf{R_c}(C_{SF,j}^{(i)})$. If the incremental MAI coefficients of any two candidate codes tie, go to the next stage. Otherwise, the smallest sum of the incremental MAI coefficients in the set of $\mathbf{R_c}(C_{SF,j}^{(i)})$ is selected. The decision rules are detailed as follows.

a) For the nth code in $\mathbf{R_c}(C_{SF,j}^{(i)})$ denoted by $C_n \in \mathbf{R_c}(C_{SF,j}^{(i)})$, we calculate its increment of the MAI coefficient $[\Delta_\kappa(C_n)]$ if $C_{SF,j}^{(i)}$ is chosen.

b) Denote $\Delta_\kappa[\mathbf{R_c}(C_{SF,j}^{(i)})]$ as the sum of $\Delta_\kappa(C_n)$ for $C_n \in \mathbf{R_c}(C_{SF,j}^{(i)})$. Then, we can have

$$\Delta_\kappa\left(\mathbf{R_c}\left(C_{SF,j}^{(i)}\right)\right) = \sum_{C_n \in \mathbf{R_c}\left(C_{SF,j}^{(i)}\right)} \Delta_\kappa(C_n). \tag{16}$$

c) Select the codes with $\mathbf{min}\{\Delta_\kappa[\mathbf{R_c}(C_{SF,j}^{(i)})]\}$.

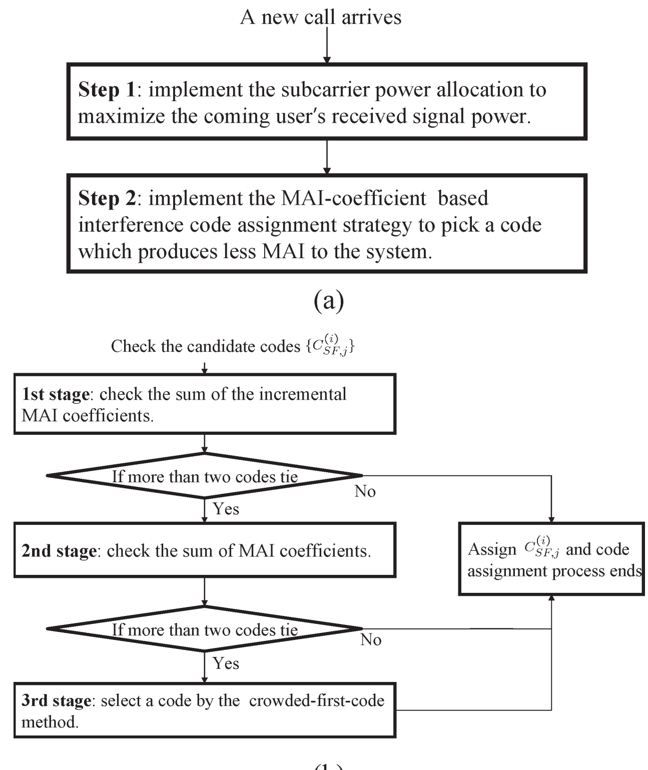

Fig. 5. Flow chart of the joint SPA and interference avoidance code assignment strategy. (a) Two steps of the joint SPA and code assignment strategy. (b) Three stages of the interference code assignment strategy.

$$\gamma = P_o G_o \sum_{v=1}^{M} |\alpha_{o,s,v}|^4 \left\{ \underbrace{2 \sum_{v=1}^{M} \sum_{k=1}^{K_{\mathbf{A}}} \sum_{\ell=0}^{L_k^{(\mathbf{A})}-1} \frac{R_k^{(\mathbf{A})}}{R_o} \frac{|\alpha_{o,s,v}|^4}{\left(L_k^{(\mathbf{A})}\right)^2} \mathrm{E}\left[\frac{\left|\alpha_{k,s,v}^{(\mathbf{A})}\right|^4}{\sum_{i=1}^{M}\left|\alpha_{k,s,i}^{(\mathbf{A})}\right|^4}\right] P_o G_o}_{\text{MAI}} + \underbrace{P_N \sum_{v=1}^{M} |\alpha_{s,v}|^2}_{\text{noise}} \right\}^{-1} \tag{12}$$

d) If there is only one code with $\mathbf{min}\{\Delta_\kappa[\mathbf{R_c}(C_{SF,j}^{(i)})]\}$, the code assignment process ends, otherwise, go to the next stage.

Stage 2) Compare the sum of the MAI coefficients of the codes in $\mathbf{R_c}(C_{SF,\beta}^{(\alpha)})$, where $\{C_{SF,\beta}^{(\alpha)}\}$ is the code set with the same sum of increment of the MAI coefficients in the first stage. Then, assign the code with the smallest sum of MAI coefficients. If two candidates tie, go to the next stage. The rules in the second stage are detailed as follows.

a) Similar to the first stage, we calculate the MAI coefficient of the nth codes in $\mathbf{R_c}(C_{SF,\beta}^{(\alpha)})$, which is denoted by $\kappa(C_n)$.

b) Denote $\kappa[\mathbf{R_c}(C_{SF,\beta}^{(\alpha)})]$ as the sum of $\kappa(C_n)$, where $C_n \in \mathbf{R_c}(C_{SF,\beta}^{(\alpha)})$. Then, we can have

$$\kappa\left(\mathbf{R_c}\left(C_{SF,\beta}^{(\alpha)}\right)\right) = \sum_{C_n\in\mathbf{R_c}\left(C_{SF,\beta}^{(\alpha)}\right)} \kappa(C_n). \quad (17)$$

c) Pick the codes with $\mathbf{min}\{\kappa[\mathbf{R_c}(C_{SF,\beta}^{(\alpha)})]\}$.

d) If there is only one code with $\mathbf{min}\{\kappa[\mathbf{R_c}(C_{SF,\beta}^{(\alpha)})]\}$, the code assignment process ends, otherwise, go to the last stage.

Stage 3) Select a code in $\{C_{SF,\delta}^{(\gamma)}\}$ according to the crowded-first-code principle, as suggested in [23], where $\{C_{SF,\delta}^{(\gamma)}\}$ is the code set with the same sum of MAI coefficients in the second stage.

B. Example

Consider a situation in which a user requests a code with a time-domain spreading factor $SF = 8$. Referring to Fig. 2, the candidate codes for this request are $\{C_{8,6}^{(1)}, C_{8,7}^{(1)}, C_{8,8}^{(1)}, C_{8,7}^{(4)}, C_{8,8}^{(4)}, C_{8,1}^{(2)}, C_{8,2}^{(2)}, C_{8,1}^{(4)}, C_{8,2}^{(4)}\}$. Based on the definition of the related codes, we can divide the candidate codes into three groups, as shown in Fig. 2. To be more specific, Groups 1 to 3 are affected by the interference from the users with the allocated codes $\{C_{4,3}^{(2)}, C_{2,2}^{(3)}, C_{4,3}^{(4)}\}$, $\{C_{4,4}^{(2)}, C_{2,2}^{(3)}\}$, and $\{C_{2,1}^{(1)}, C_{4,1}^{(3)}\}$, respectively. Now, we give an example to illustrate the joint SPA and interference avoidance code assignment strategy. Consider codes $\{C_{8,6}^{(1)}, C_{8,7}^{(1)}, C_{8,1}^{(2)}\}$ to be the representatives of their respective groups in the 2-D code tree in Fig. 2. In other words, the MAI coefficients of codes within a group are the same.

SPA Procedure: As mentioned in Section V-A, the first step of the proposed scheme is to allocate the power to subcarriers according to (10).

Interference Avoidance Code Assignment: Now, the interference avoidance code assignment strategy is applied to select a code that produces less MAI.

a) Compare the increment of the MAI coefficient $[\sum \delta_\kappa(\cdot)]$*:* First, we compare the increment of the MAI coefficient $\sum \Delta_\kappa(\cdot)$. According to the definition of the related codes, one can find that the related codes for code $C_{8,6}^{(1)}$ are $C_{4,3}^{(2)}, C_{2,2}^{(3)}$, and $C_{4,3}^{(4)}$. Thus, we have

$$\mathbf{R}_c\left(C_{8,6}^{(1)}\right) = \left\{C_{8,6}^{(1)}, C_{4,3}^{(2)}, C_{2,2}^{(3)}, C_{4,3}^{(4)}\right\}. \quad (18)$$

Based on (15), the incurred MAI coefficient $\Delta_\kappa[\mathbf{R}_c(C_{8,6}^{(1)})]$ after allocating code $C_{8,6}^{(1)}$ is equal to

$$\begin{aligned}\Delta_\kappa\left[\mathbf{R}_c\left(C_{8,6}^{(1)}\right)\right] &= \sum_{C_n\in\mathbf{R}_c\left(C_{8,6}^{(1)}\right)} \Delta_\kappa(C_n)\\ &= \Delta_\kappa\left(C_{8,6}^{(1)}\right) + \Delta_\kappa\left(C_{4,3}^{(2)}\right)\\ &\quad + \Delta_\kappa\left(C_{2,2}^{(3)}\right) + \Delta_\kappa\left(C_{4,3}^{(4)}\right)\\ &= 4.25\end{aligned} \quad (19)$$

where

$$\begin{aligned}\Delta_\kappa\left(C_{8,6}^{(1)}\right) &= \mathbf{min}\left(1, \frac{R_{4,3}^{(2)}}{R_{8,6}^{(1)}}\right) + \mathbf{min}\left(1, \frac{R_{2,2}^{(3)}}{R_{8,6}^{(1)}}\right)\\ &\quad + \mathbf{min}\left(1, \frac{R_{4,3}^{(4)}}{R_{8,6}^{(1)}}\right)\\ &= \mathbf{min}\left(1, \frac{2}{1}\right) + \mathbf{min}\left(1, \frac{4}{1}\right) + \mathbf{min}\left(1, \frac{2}{1}\right) = 3\end{aligned} \quad (20)$$

$$\Delta_\kappa\left(C_{4,3}^{(2)}\right) = \mathbf{min}\left(1, \frac{R_{8,6}^{(1)}}{R_{4,3}^{(2)}}\right) = \frac{1}{2} \quad (21)$$

$$\Delta_\kappa\left(C_{2,2}^{(3)}\right) = \mathbf{min}\left(1, \frac{R_{8,6}^{(1)}}{R_{2,2}^{(3)}}\right) = \frac{1}{4} \quad (22)$$

$$\Delta_\kappa\left(C_{4,3}^{(4)}\right) = \mathbf{min}\left(1, \frac{R_{8,6}^{(1)}}{R_{4,3}^{(4)}}\right) = \frac{1}{2}. \quad (23)$$

Similarly, we can obtain $\Delta_\kappa[\mathbf{R}_c(C_{8,7}^{(1)})] = 2.75$ and $\Delta_\kappa[\mathbf{R}_c(C_{8,1}^{(2)})] = 2.75$. Because $\Delta_\kappa[\mathbf{R}_c(C_{8,7}^{(1)})] = \Delta_\kappa[\mathbf{R}_c(C_{8,1}^{(2)})] = 2.75$, the code assignment enters the second stage to compare codes $C_{8,7}^{(1)}$ and $C_{8,1}^{(2)}$.

b) Compare the sum of the MAI coefficient $[\sum \kappa(\cdot)]$*:* In this stage, the sum of the MAI coefficients of related codes $\sum \kappa(\cdot)$ for codes $C_{8,7}^{(1)}$ and $C_{8,1}^{(2)}$ are compared.

(a) Calculate $\kappa[\mathbf{R}_c(C_{8,7}^{(1)})]$: According to the definition of the related codes, we can find that $\mathbf{R}_c(C_{8,7}^{(1)}) = \mathbf{R}_c(C_{4,4}^{(2)}) = \{C_{8,7}^{(1)}, C_{4,4}^{(2)}, C_{2,2}^{(3)}\}$. Similarly, we have $\mathbf{R}_c(C_{2,2}^{(3)}) = \{C_{8,5}^{(1)}, C_{8,7}^{(1)}, C_{4,3}^{(2)}, C_{4,4}^{(2)}, C_{4,3}^{(4)}, C_{2,2}^{(3)}\}$. Then, it follows that

$$\begin{aligned}\kappa\left[\mathbf{R}_c\left(C_{8,7}^{(1)}\right)\right] &= \sum_{C_n\in\mathbf{R}_c\left(C_{8,7}^{(1)}\right)} \kappa(C_n)\\ &= \kappa\left(C_{8,7}^{(1)}\right) + \kappa\left(C_{4,4}^{(2)}\right) + \kappa\left(C_{2,2}^{(3)}\right)\\ &= 5.5\end{aligned} \quad (24)$$

where

$$\kappa\left(C_{8,7}^{(1)}\right) = \mathbf{min}\left(1, \frac{R_{4,4}^{(2)}}{R_{8,7}^{(1)}}\right) + \mathbf{min}\left(1, \frac{R_{2,2}^{(3)}}{R_{8,7}^{(1)}}\right)$$
$$= \mathbf{min}\left(1, \frac{2}{1}\right) + \mathbf{min}\left(1, \frac{4}{1}\right) = 2 \qquad (25)$$

$$\kappa\left(C_{4,4}^{(2)}\right) = \mathbf{min}\left(1, \frac{R_{8,7}^{(1)}}{R_{4,4}^{(2)}}\right) + \mathbf{min}\left(1, \frac{R_{2,2}^{(3)}}{R_{4,4}^{(2)}}\right)$$
$$= \mathbf{min}\left(1, \frac{1}{2}\right) + \mathbf{min}\left(1, \frac{4}{2}\right) = 1.5 \qquad (26)$$

$$\kappa\left(C_{2,2}^{(3)}\right) = \mathbf{min}\left(1, \frac{R_{8,5}^{(1)}}{R_{2,2}^{(3)}}\right) + \mathbf{min}\left(1, \frac{R_{8,7}^{(1)}}{R_{2,2}^{(3)}}\right) + \mathbf{min}\left(1, \frac{R_{4,3}^{(2)}}{R_{2,2}^{(3)}}\right) + \mathbf{min}\left(1, \frac{R_{4,4}^{(2)}}{R_{2,2}^{(3)}}\right) + \mathbf{min}\left(1, \frac{R_{4,3}^{(4)}}{R_{2,2}^{(3)}}\right)$$
$$= \mathbf{min}\left(1, \frac{1}{4}\right) + \mathbf{min}\left(1, \frac{1}{4}\right) + \mathbf{min}\left(1, \frac{1}{2}\right) + \mathbf{min}\left(1, \frac{1}{2}\right) + \mathbf{min}\left(1, \frac{1}{2}\right) = 2. \qquad (27)$$

(b) Calculate $\kappa[\mathbf{R}_c(C_{8,1}^{(2)})]$: Referring to Fig. 2, it is clear that

$$\mathbf{R}_c\left(C_{8,1}^{(2)}\right) = \mathbf{R}_c\left(C_{4,1}^{(3)}\right) = \left\{C_{8,1}^{(2)}, C_{4,1}^{(3)}, C_{2,1}^{(1)}\right\} \qquad (28)$$

$$\mathbf{R}_c\left(C_{2,1}^{(1)}\right) = \left\{C_{8,1}^{(2)}, C_{8,3}^{(2)}, C_{8,4}^{(2)}, C_{4,1}^{(3)}, C_{4,2}^{(3)}, C_{8,3}^{(4)}, C_{8,4}^{(4)}, C_{2,1}^{(1)}\right\}. \qquad (29)$$

Similar to (24), we can have

$$\kappa\left[\mathbf{R}_c\left(C_{8,1}^{(2)}\right)\right] = \sum_{C_n \in \mathbf{R}_c\left(C_{8,1}^{(2)}\right)} \kappa(C_n)$$
$$= \kappa\left(C_{8,1}^{(2)}\right) + \kappa\left(C_{4,1}^{(3)}\right) + \kappa\left(C_{2,1}^{(1)}\right)$$
$$= 5.75 \qquad (30)$$

where $\kappa[C_{8,1}^{(2)})] = 2$, $\kappa[C_{4,1}^{(3)})] = 1.5$, and $\kappa[C_{2,1}^{(1)})] = 2.25$ can be calculated by the same approach as (27). Because code $C_{8,7}^{(1)}$ will have less total MAI in the set of its related codes than code $C_{8,1}^{(2)}$, it is chosen to serve the requested call.

VI. Simulation Results

In this section, we demonstrate the effectiveness of the proposed joint SPA and code assignment strategy. We first show the advantages of using the proposed SPA mechanism. Then, with the SPA mechanism, we illustrate the impact of an MAI-coefficient-based interference code assignment strategy by comparing the various code assignment strategies [random assignment (RM), pure crowded-first-code assignment (CF) without considering MAI, and the interference avoidance assignment (IA + CF) methods] in terms of the received E_b/N_0 and call admission rate.

A. Simulation Setup

1) Simulation Environment: In the simulation, we consider a downlink MC-DS-CDMA in a single-cell environment. Following the assumptions in [7] and [12], the subcarriers carrying the same data bits are assumed to experience independent flat Rayleigh fading. The background noise is modeled by white Gaussian noise with a double-sided power spectrum density of $N_0/2$ and a transmitting $E_b/N_0 = 12$ dB. A new call is modeled by a Poisson arrival process with the arrival rate (λ) of 1/2 per time unit and the departure rate (μ) selecting from the set $\{1/32, 1/48, 1/64, 1/80, 1/96, 1/112, 1/144, 1/176\}$. Thus, there are, on average, $\lambda/\mu = 16 \sim 88$ active calls in the system. With $U = 128$ parallel substreams, the frequency-domain spreading factor (M) is 8, and the time-domain spreading factors (SFs) are 4, 8, 16, or 32. Each call requests a code of $8R$ ($SF = 4$), $4R$ ($SF = 8$), $2R$ ($SF = 16$), or R ($SF = 32$) with a probability according to the code traffic pattern $[1 \quad 1 \quad 2 \quad 8]$, where R is the basic data rate. A code traffic pattern of $[a \quad b \quad c \quad d]$ means that the times of requesting data rates $8R$, $4R$, $2R$, and R are proportional to $a : b : c : d$, respectively. The data rate of each user is fixed during its call holding time. To clearly indicate the traffic load brought by the active calls with different data rates, we define an effective traffic load in the following. With the time-domain spreading factor selecting from $SF = [4 \quad 8 \quad 16 \quad 32]$ and the code traffic pattern of $[a \quad b \quad c \quad d]$, the effective traffic load (ρ) is defined as

$$\rho = \frac{\lambda}{\mu} \times \frac{8R \times a + 4R \times b + 2R \times c + R \times d}{a + b + c + d} \times \frac{1}{32R}. \qquad (31)$$

For $\lambda = 1/2$ and $\mu = 1/80$ and the code traffic pattern $[1 \quad 1 \quad 2 \quad 8]$, the effective traffic load ρ is 250% of the utilization of the time-domain resources.

2) Call Admission Control: In the call admission control, we consider the average received E_b/N_0. For an MAI coefficient (κ), the average received E_b/N_0 can be calculated by taking the average of (42) over the M subcarriers' fading channels. A incoming call is blocked if accepting this new call decreases the signal quality of any active calls in the system below the required received $E_b/N_o = 5$ dB. We simulate 10 000 incoming calls for each combination of λ and μ.

3) Code Assignment Strategy: Consider a call request for a code with rate $2^k R$, where k is an integer ranging from 0 to 3. Then, a code assignment strategy should be implemented to pick a candidate code to accommodate this new coming call. A candidate code is defined as a free code with rate $2^k R$, and its ancestor and descent codes are not used. In this paper, we consider three code assignment methods, namely RM, CF, and IA + CF. Now, we introduce the RM and CF methods.

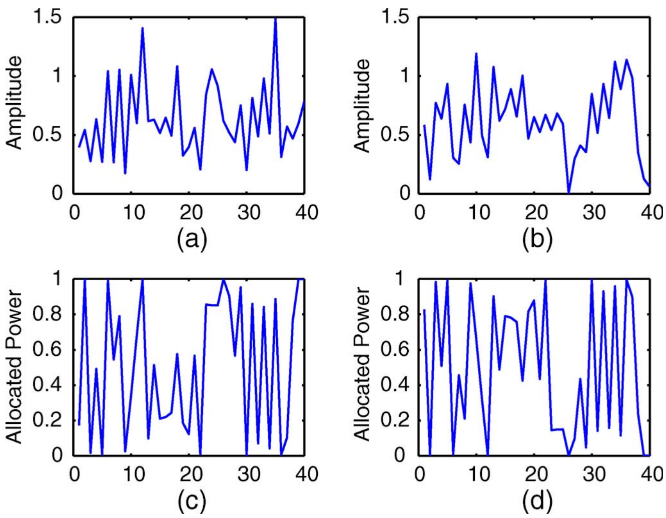

Fig. 6. Example of the variations of the fading channels at different subcarriers and the corresponding SPAs, where the number of subcarriers is $M = 2$, and the transmission power constraint is $P_o = 1$. (a) Amplitude of the first subcarrier. (b) Amplitude of the second subcarrier. (c) Allocated power to the first subcarrier. (d) Allocated power to the second subcarrier.

RM: If there is one or more candidate codes in the 2-D code tree, the RM method randomly selects a code without considering the code tree structure and the impact of MAI.

CF: If there is one or more candidate codes in the 2-D code tree, the CF method picks a code whose ancestor code has the fewest free codes and thereby leaves more space for future high-rate users to increase the call admission rate [23]. Note that the CF method considers the code tree structure but not the impact of MAI.

B. Effect of SPA

Fig. 6 shows an illustrative example of the variations of the channels at different subcarriers and the corresponding SPAs, where the number of subcarriers is $M = 2$, and the transmission power constraint is $P_o = 1$. As shown in the figure, according to the rule of (10) and (11), the power allocated to a subcarrier is proportional to the amplitude of that subcarrier. Moreover, the sum of the power allocated to the first and second subcarriers is equal to $P_o = 1$.

Fig. 7(a)–(c) compare the proposed joint SPA and code assignment strategy $(\mathrm{IA} + \mathrm{CF} + \mathrm{SPA})$ with the pure interference avoidance code assignment strategy $(\mathrm{IA} + \mathrm{CF})$ in terms of the (a) average received E_b/N_0, (b) average call admission rate, and (c) standard deviation (STD) of the received E_b/N_0 with various effective traffic loads. One can see that with the help of SPA, the proposed $\mathrm{IA} + \mathrm{CF} + \mathrm{SPA}$ method performs much better than the pure $\mathrm{IA} + \mathrm{CF}$ method both in terms of the average received E_b/N_0 and the average call admission rate. Furthermore, the advantage of using the proposed SPA mechanism grows as the traffic load increases. Referring to Fig. 7(a), from the average received E_b/N_0 aspect, the improvement by using the proposed SPA mechanism increases from 0.3 to 1.9 dB for $\rho = 1.5$ and 3.5, respectively. As shown in Fig. 7(b) as well, the improvement of the call admission rises from 4% to 10% for $\rho = 1.5$ and 3.5, respectively. Moreover, thanks to SPA, the STD of the received E_b/N_0 can be significantly reduced, as shown in Fig. 7(c). At $\rho = 1.5$, the STD of the received E_b/N_0 reduces from 2.6 to 1.4 in the decibel domain. This is because SPA can make the received signal quality more robust against the fading channel. One should note that the STD of the received E_b/N_0 for both $\mathrm{IA} + \mathrm{CF}$ and $\mathrm{IA} + \mathrm{CF} + \mathrm{SPA}$

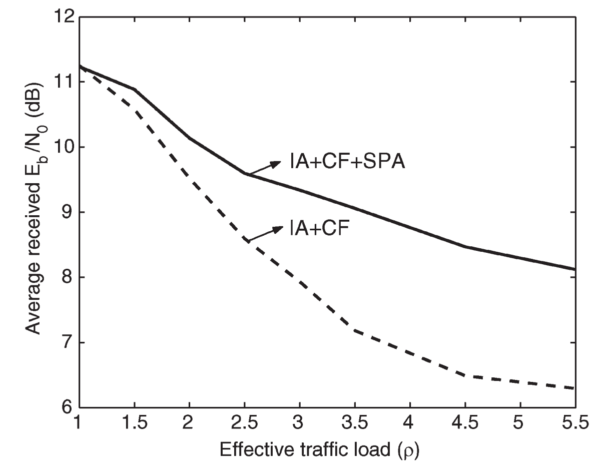

(a) Average received $E_b=N_0$ (dB)

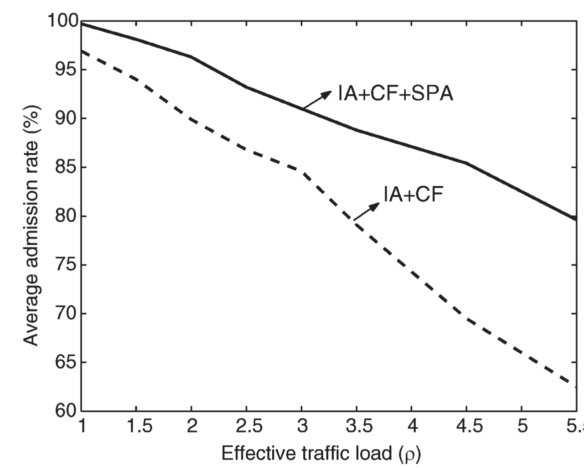

(b) Average admission rate (%)

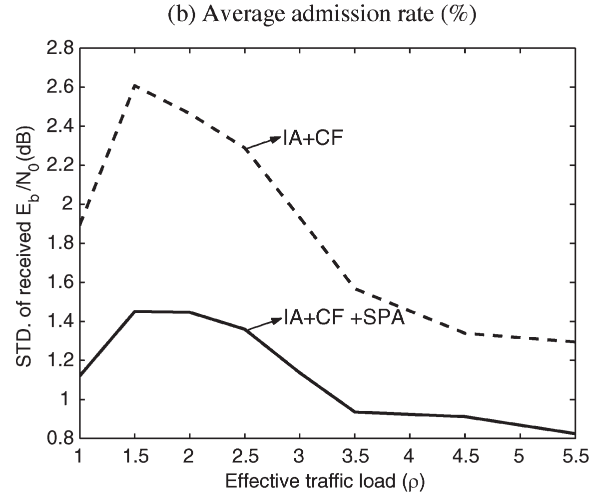

(c) STD. of received $E_b=N_0$ (dB)

Fig. 7. Comparison between the proposed joint SPA and code assignment strategy and the pure interference avoidance code assignment strategy in terms of the (a) average received E_b/N_0, (b) call admission rate, and (c) STD of the received E_b/N_0 with various effective traffic loads.

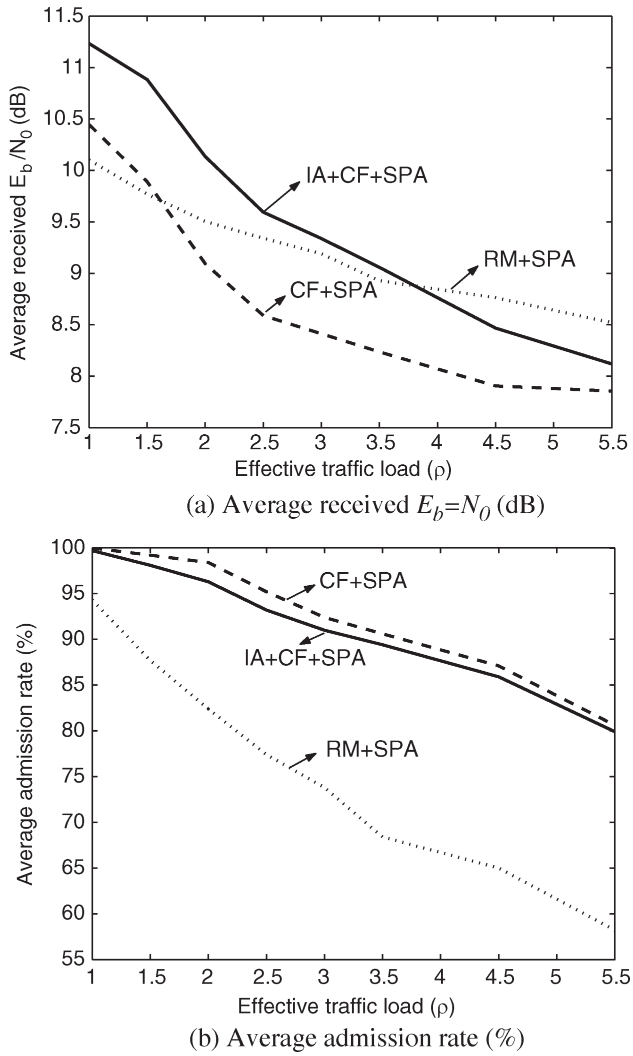

(a) Average received E_b=N_0 (dB)

(b) Average admission rate (%)

Fig. 8. Comparison of (a) the average received E_b/N_0 and (b) the call admission rate against the effective traffic load for the proposed joint SPA and code assignment (IA + CF + SPA), SPA-aided crowded-first-code assignment (CF + SPA), and SPA-aided random assignment (RM + SPA) strategies.

increases in the range of $1 \leq \rho \leq 1.5$ and begins to decrease as ρ increases. When the traffic load is light at $\rho = 1$, the interference avoidance code assignment strategy can effectively select codes for all users without producing extra MAI. However, as the traffic load increases to $\rho = 1.5$, some users may use codes experiencing few interferers, whereas some other users may not. As the traffic load continues to grow, all the active codes may have a similar amount of interference.

C. Effect of Interference Avoidance Code Assignment Strategy

Fig. 8(a) and (b) compare the average received E_b/N_0 and call admission rate against the effective traffic load for the proposed joint SPA and code assignment (IA + CF + SPA), SPA-aided crowded-first assignment (CF + SPA), and SPA-aided random assignment (RM + SPA) strategies. First, in terms of received E_b/N_0, IA + CF + SPA performs better than RM + SPA for $1 \leq \rho < 4$, whereas in the higher traffic load region of $\rho \geq 4$, the received E_b/N_0 of IA + CF + SPA is lower than that of RM + SPA. With higher traffic load, IA + CF + SPA can accommodate more users than RM + SPA because IA + CF + SPA skillfully assigns code channels to avoid producing excessive MAI, whereas RM + SPA blocks call requests owing to the careless code assignment. Thus, with more users in the system, a user tends to be affected by more interferers, which results in the lower E_b/N_0 for the IA + CF + SPA method.

Second, for the same reason, the received E_b/N_0 of the CF + SPA method becomes lower than RM + SPA in the region of $\rho > 1.5$. Third, the RM + SPA method performs the worst in terms of the call admission rate because it randomly assigns codes without considering the code tree structure or MAI. Fourth, comparing IA + CF + SPA and CF + SPA, the IA + CF + SPA method can have a higher received E_b/N_0 than the CF + SPA method, whereas the call admission rate of the IA + CF + SPA is slightly lower than the CF + SPA method. For example, the average received E_b/N_0 at $\rho = 2.5$ is 8.6 and 9.6 dB for CF + SPA and IA + CF + SPA, respectively. However, the call admission rate of the IA + CF + SPA is 2% lower than CF + SPA. Note that the CF + SPA method can make the tree structure of the allocated codes more compact, thereby gathering more larger code resources for higher rate users and having a higher admission rate. However, the IA + CF + SPA method aims to first avoid MAI before applying the CF method. Moreover, for the region of $1.5 \leq \rho \leq 4$, the CF + SPA method has the poorest E_b/N_0 performance, even compared to the RM + SPA method. This also justifies the advantages of the IA + CF + SPA method.

VII. Conclusion

In this paper, we have proposed a joint SPA and code assignment strategy for the multirate synchronous MC-DS-CDMA with TF-domain spreading. In the proposed joint scheme, we first optimized the received signal power using an SPA mechanism. Then, an MAI-coefficient-aided interference avoidance code assignment strategy was applied to eliminate MAI. The MAI coefficient was used to predict the quantity of the MAI imposed on each code channel. Through simulations and analysis, we have demonstrated that the proposed joint SPA and code assignment method can simultaneously effectively enhance the received E_b/N_0 and maintain a high call admission rate. Interesting future research topics include the application of the concept of the MAI coefficients to the MC-DS-CDMA system when combined with the multiple-input–multiple-output antenna technology [13] or power control mechanisms [24].

Appendix A

In this Appendix, we derive (12). To facilitate the calculation of $I_{k,s,v}^{(\mathbf{X})}$, we consider two scenarios according to the relation between T_o (the bit duration of the reference user) and $T_k^{(\mathbf{X})}$ (the bit duration of the interfering user k in group $\mathbf{X}$).

MAI From High Data Rate Users ($T_o > T_k^{(\mathbf{X})}$)

In this case, the ratio of bit duration of the desired users to the interfering user of group $\mathbf{X} \in \{\mathbf{A}, \mathbf{B}, \mathbf{C}\}$ can be written as $L_k^{(\mathbf{X})} = T_o/T_k^{(\mathbf{X})}$, where $L_k^{(\mathbf{X})}$ is a positive integer. Rewrite (4) as

$$\begin{aligned} I_{k,s,v}^{(\mathbf{X})} &= \sqrt{P_{k,s,v}^{(\mathbf{X})}} \frac{\alpha_{o,s,v}\beta_{o,s,v}c_k^{(\mathbf{X})}[v]c_o[v]}{T_o} \int_0^{T_o} b_{k,s}^{(\mathbf{X})}(t) \\ &\quad \times g_k^{(\mathbf{X})}(t)g_o(t)dt \\ &= \sqrt{P_{k,s,v}^{(\mathbf{X})}} \frac{\alpha_{o,s,v}\beta_{o,s,v}c_k^{(\mathbf{X})}[v]c_o[v]}{L_k^{(\mathbf{X})}T_k^{(\mathbf{X})}} \\ &\quad \times \sum_{\ell=0}^{L_k^{(\mathbf{X})}-1} b_{k,s}^{(\mathbf{X})}[\ell] \int_0^{T_k^{(\mathbf{X})}} g_k^{(\mathbf{X})}(t)g_o(t)dt. \end{aligned} \tag{32}$$

Based on the definition of the user group in Section II-B, we can have $I_{k,s,v}^{(\mathbf{B})} = I_{k,s,v}^{(\mathbf{C})} = 0$ because $\int_0^{T_k^{(\mathbf{B})}} g_k^{(\mathbf{B})}(t)g_o(t)dt = 0$, and $\int_0^{T_k^{(\mathbf{C})}} g_k^{(\mathbf{C})}(t)g_o(t)dt = 0$. That is, the time-domain spreading codes of the users in groups $\mathbf{B}$ and $\mathbf{C}$ are orthogonal to the reference user. Recall that $b_{k,s}^{(\mathbf{A})}[\ell] = \pm 1$ with equal probability. Thus, it follows that

$$\frac{b_{k,s}^{(\mathbf{A})}[\ell]}{T_k^{(\mathbf{A})}} \int_0^{T_k^{(\mathbf{A})}} g_k^{(\mathbf{A})}(t)g_o(t)dt = \pm 1 \tag{33}$$

with equal probability. Consequently, (32) can be simplified as

$$I_{k,s,v}^{(\mathbf{A})} = \sqrt{P_{k,s,v}^{(\mathbf{A})}} \frac{\alpha_{o,s,v}\beta_{o,s,v}c_k^{(\mathbf{A})}[v]c_o[v]}{L_k^{(\mathbf{A})}} \sum_{\ell=0}^{L_k^{(\mathbf{A})}-1} \Delta[\ell] \tag{34}$$

where $\Delta[\ell] = \pm 1$ with equal probability.

MAI From Low Data Rate Users ($T_o \leq T_k^{(\mathbf{X})}$)

In this case, we express $I_{k,s,v}^{(\mathbf{X})}$ as

$$\begin{aligned} I_{k,s,v}^{(\mathbf{X})} &= \sqrt{P_{k,s,v}^{(\mathbf{X})}} \frac{\alpha_{o,s,v}\beta_{o,s,v}c_k^{(\mathbf{X})}[v]c_o[v]}{T_o} \int_0^{T_o} b_{k,s}^{(\mathbf{X})}(t) \\ &\quad \times g_k^{(\mathbf{X})}(t)g_o(t)dt \\ &= \sqrt{P_{k,s,v}^{(\mathbf{X})}} \frac{\alpha_{o,s,v}\beta_{o,s,v}c_k^{(\mathbf{X})}[v]c_o[v]}{T_o} b_{k,s}^{(\mathbf{X})}[0] \\ &\quad \times \int_0^{T_o} g_k^{(\mathbf{X})}(t)g_o(t)dt. \end{aligned} \tag{35}$$

Similar to the case of the MAI from high data rate users, we have $I_{k,v}^{(\mathbf{B})} = I_{k,v}^{(\mathbf{C})} = 0$, and

$$\frac{b_{k,s}^{(\mathbf{A})}[0]}{T_o} \int_0^{T_o} g_k^{(\mathbf{A})}(t)g_o(t)dt = \pm 1. \tag{36}$$

Thus, it follows that

$$I_{k,s,v}^{(\mathbf{A})} = \sqrt{P_{k,s,v}^{(\mathbf{A})}}\alpha_{o,s,v}\beta_{o,s,v}c_k^{(\mathbf{A})}[v]c_o[v]\Delta[0] \tag{37}$$

where $\Delta[0]$ is defined in (34). Note that (37) is the special case of (34). Specifically, we can obtain (37) by letting $L_k^{(\mathbf{A})} = 1$ in (34).

Let $\beta_{o,s,v} = \alpha_{o,s,v}^*$ for the maximum ratio combining scheme. With $I_{k,v}^{(\mathbf{B})} = I_{k,v}^{(\mathbf{C})} = 0$, we substitute (10), (11), (34), and (37) into (5) and obtain

$$\begin{aligned} Y_{o,s} = \sqrt{\frac{P_o}{2}}T_o \Bigg\{ & b_{o,s}[0] \frac{\sum_{v=1}^M |\alpha_{o,s,v}|^4}{\sqrt{\sum_{i=1}^M |\alpha_{o,s,i}|^4}} \\ & + \sum_{k=1}^{K_\mathbf{A}} \sum_{v=1}^{M} \sum_{\ell=0}^{L_k^{(\mathbf{A})}-1} \sqrt{\frac{P_k^{(\mathbf{A})}}{P_o}} \\ & \times \frac{\left|\alpha_{k,s,v}^{(\mathbf{A})}\right|^2 |\alpha_{o,s,v}|^2 c_k^{(\mathbf{A})}[v]c_o[v]}{\sqrt{\sum_{i=1}^M \left|\alpha_{k,s,i}^{(\mathbf{A})}\right|^4} L_k^{(\mathbf{A})}} \Delta[\ell] \\ & + \frac{1}{\sqrt{P_o}} \sum_{v=1}^M n_{s,v} \Bigg\}. \end{aligned} \tag{38}$$

Following [20], we assume that the MAI can be approximated by a zero-mean Gaussian-distributed random variable. Thus, the normalized decision variable $Y_{o,s}$ can be modeled by a Gaussian random variable with mean

$$E[Y_{o,s}] = b_{o,s}[0]\sqrt{\sum_{v=1}^M |\alpha_{o,s,v}|^4} \tag{39}$$

and variance

$$\begin{aligned} \mathrm{Var}[Y_{o,s}] &= \sum_{v=1}^{M}\sum_{k=1}^{K_\mathbf{A}}\sum_{\ell=0}^{L_k^{(\mathbf{A})}-1} \mathrm{Var}\left[\sqrt{\frac{P_k^{(\mathbf{A})}}{P_o}} \frac{\left|\alpha_{k,s,v}^{(\mathbf{A})}\right|^2 |\alpha_{o,s,v}|^2}{\sqrt{\sum_{i=1}^M |\alpha_{k,s,i}^{(\mathbf{A})}|^4}} \right. \\ &\qquad \left. \times \frac{c_k^{(\mathbf{A})}[v]c_o[v]\Delta[\ell]}{L_k^{(\mathbf{A})}}\right] \\ &\quad + \frac{1}{2}\left(\frac{E_o}{N_0}\right)^{-1} \sum_{v=1}^M |\alpha_{o,s,v}|^2 \\ &= \sum_{v=1}^{M}\sum_{k=1}^{K_\mathbf{A}}\sum_{\ell=0}^{L_k^{(\mathbf{A})}-1} \frac{P_k^{(\mathbf{A})}}{P_o} \frac{|\alpha_{o,s,v}|^4}{\left(L_k^{(\mathbf{A})}\right)^2} \mathrm{E}\left[\frac{\left|\alpha_{k,s,v}^{(\mathbf{A})}\right|^4}{\sum_{i=1}^M \left|\alpha_{k,s,i}^{(\mathbf{A})}\right|^4}\right] \\ &\quad + \frac{1}{2}\left(\frac{E_o}{N_0}\right)^{-1} \sum_{v=1}^M |\alpha_{o,s,v}|^2. \end{aligned} \tag{40}$$

Define the received E_b/N_0 (denoted by γ) as expressed in (41), shown at the bottom of the next page,where R_o and $R_k^{(\mathbf{A})}$ are the transmission rates of the reference user and user k in group $\mathbf{A}$, respectively. Note that $E_o = P_o T_o$ and $N_0 = P_n T_c$, where P_o and P_n are the transmission power of the reference user and the noise power. As in [21] and [22], $R_k^{(\mathbf{A})}/R_o = P_k^{(\mathbf{A})}/P_o$ means that a high-rate user needs more power.

Appendix B

In this Appendix, we use the Laguerre integration to evaluate the error rate performance of the synchronous multirate MC-DS-CDMA system with TF-domain spreading when the SPA mechanism is applied. Substituting the MAI coefficient κ of (15) into the received E_b/N_0 of (12), we obtain

$$\gamma = \sum_{v=1}^{M} |\alpha_{o,s,v}|^4 \left\{ 2\kappa \mathrm{E}\left[\frac{\left|\alpha_{k,s,v}^{(\mathbf{A})}\right|^4}{\sum_{i=1}^{M} \left|\alpha_{k,s,i}^{(\mathbf{A})}\right|^4} \right] \sum_{v=1}^{M} |\alpha_{o,s,v}|^4 + \left(\frac{E_o}{N_0}\right)^{-1} \sum_{v=1}^{M} |\alpha_{o,s,v}|^2 \right\}^{-1}. \quad (42)$$

Because $|\alpha_{o,s,v}|$ and $|\alpha_{k,s,i}^{(\mathbf{A})}|$ are the amplitudes of the Rayleigh-fading channel, $|\alpha_{o,s,v}|^2$ and $|\alpha_{k,s,i}^{(\mathbf{A})}|^2$ are the exponentially distributed random variable with mean $E[|\alpha_{o,s,v}|^2] = E[|\alpha_{k,s,i}^{(\mathbf{A})}|^2] = 1$. To ease the notation, we denote $z_{ov} = |\alpha_{o,s,v}|^2$ and $z_{ki} = |\alpha_{k,s,i}^{(\mathbf{A})}|^2$. Then, the probability density function of z_{ov} and z_{kv} are expressed as

$$f_{z_{ov}}(z_{ov}) = e^{-z_{ov}} U(z_{ov}) \quad (43)$$

$$f_{z_{ki}}(z_{ki}) = e^{-z_{ki}} U(z_{ki}) \quad (44)$$

where

$$U(t) = \begin{cases} 1, & t \geq 0 \\ 0, & t < 0. \end{cases} \quad (45)$$

Then, $\mathrm{E}[|\alpha_{k,s,v}^{(\mathbf{A})}|^4/\sum_{i=1}^{M} |\alpha_{k,s,i}^{(\mathbf{A})}|^4]$ of (12) can be expressed as

$$\begin{aligned} &\mathrm{E}\left[\frac{\left|\alpha_{k,s,v}^{(\mathbf{A})}\right|^4}{\sum_{i=1}^{M} \left|\alpha_{k,s,i}^{(\mathbf{A})}\right|^4} \right] \\ &= \mathrm{E}\left[\frac{|z_{kv}|^2}{\sum_{i=1}^{M} |z_{ki}|^2} \right] \\ &= \int_0^\infty \cdots \int_0^\infty \frac{|z_{kv}|^2}{\sum_{i=1}^{M} |z_{ki}|^2} f_{z_{k1}}(z_{k1}) \cdots \\ &\quad f_{z_{kM}}(z_{kM}) d_{z_{k1}} \cdots d_{z_{kM}} \\ &= \int_0^\infty \cdots \int_0^\infty \frac{|z_{kv}|^2}{\sum_{i=1}^{M} |z_{ki}|^2} e^{-z_{k1}} \cdots e^{-z_{kM}} d_{z_{k1}} \cdots d_{z_{kM}}. \end{aligned} \quad (46)$$

Due to the tediousness and complexity of the calculations, we suggest the application of the Laguerre polynomial approach of [25] to calculate (46). Based on the Laguerre polynomial approach, the integration for a function $q(x)e^{-x}$ can be computed by

$$\int_0^\infty q(x) e^{-x} dx = \sum_{i=1}^{H} \omega_i q(x_i) \quad (47)$$

where x_i and ω_i are the abscissas and the weight factor of the Laguerre polynomials with order H, respectively. By applying the Laguerre integration into (46), we can calculate $\mathrm{E}[|\alpha_{k,s,v}^{(\mathbf{A})}|^4/\sum_{i=1}^{M} |\alpha_{k,s,i}^{(\mathbf{A})}|^4]$ as

$$\mathrm{E}\left[\frac{\left|\alpha_{k,s,v}^{(\mathbf{A})}\right|^4}{\sum_{i=1}^{M} \left|\alpha_{k,s,i}^{(\mathbf{A})}\right|^4} \right] = \sum_{i_1=1}^{H} \cdots \sum_{i_M=1}^{H} w_{k1,i_1} \cdots w_{kM,i_M} \frac{|z_{kv,i_v}|^2}{\sum_{j=1}^{M} |z_{kj,i_j}|^2}. \quad (48)$$

$$\begin{aligned} \gamma &= \frac{E^2[Y_{o,s}]}{2\mathrm{Var}[Y_{o,s}]} \\ &= \sum_{v=1}^{M} |\alpha_{o,s,v}|^4 \left\{ 2 \sum_{v=1}^{M} \sum_{k=1}^{K_{\mathbf{A}}} \sum_{\ell=0}^{L_k^{(\mathbf{A})}-1} \frac{P_k^{(\mathbf{A})}}{P_o} \frac{|\alpha_{o,s,v}|^4}{\left(L_k^{(\mathbf{A})}\right)^2} \mathrm{E}\left[\frac{\left|\alpha_{k,s,v}^{(\mathbf{A})}\right|^4}{\sum_{i=1}^{M} \left|\alpha_{k,s,i}^{(\mathbf{A})}\right|^4} \right] + \left(\frac{E_o}{N_0}\right)^{-1} \sum_{v=1}^{M} |\alpha_{o,s,v}|^2 \right\}^{-1} \\ &= P_o G_o \sum_{v=1}^{M} |\alpha_{o,s,v}|^4 \left\{ \underbrace{2 \sum_{v=1}^{M} \sum_{k=1}^{K_{\mathbf{A}}} \sum_{\ell=0}^{L_k^{(\mathbf{A})}-1} \frac{R_k^{(\mathbf{A})}}{R_o} \frac{|\alpha_{o,s,v}|^4}{\left(L_k^{(\mathbf{A})}\right)^2} \mathrm{E}\left[\frac{\left|\alpha_{k,s,v}^{(\mathbf{A})}\right|^4}{\sum_{i=1}^{M} \left|\alpha_{k,s,i}^{(\mathbf{A})}\right|^4} \right] P_o G_o}_{\text{MAI}} + \underbrace{P_n \sum_{v=1}^{M} |\alpha_{s,v}|^2}_{\text{noise}} \right\}^{-1} \end{aligned} \quad (41)$$

For a binary phase-shift keying modulation with coherent detection, the conditional error probability for the given $\alpha_{o,s,v}$ is equal to

$$P(e|\alpha_{o,s,1},\ldots,\alpha_{o,s,M}) = Q(\sqrt{2\gamma}) \tag{49}$$

where $Q(x)=(1/\sqrt{2\pi})\int_x^\infty e^{-t^2/2}dt$. Recall that $z_{ov} = |\alpha_{o,s,v}|^2$. Hence, the total error probability can be expressed as

$$\begin{aligned} P(e) &= \int_0^\infty \cdots \int_0^\infty Q\left(\sqrt{2\gamma}|z_{o1},\ldots,z_{oM}\right) \\ &\quad \times f_{z_{o1}}(z_{o1})\cdots f_{z_{oM}}(z_{oM})dz_{o1}\cdots\, dz_{oM} \\ &= \int_0^\infty \cdots \int_0^\infty Q\left(\sqrt{2\gamma}|z_{o1},\ldots,z_{oM}\right) \\ &\quad \times e^{-z_{o1}}\cdots\, e^{-z_{oM}}dz_{o1}\cdots\, dz_{oM}. \end{aligned} \tag{50}$$

By applying the Laguerre integration into (50), we can further simplify the total error probability $P(e)$ as

$$\begin{aligned} P(e) = \sum_{i_1=1}^{H}\cdots\sum_{i_M=1}^{H} w_{o1,i_1}\times\cdots\times w_{oM,i_M} \\ \times Q\left(\sqrt{2\gamma}|z_{o1,i_1},\ldots,z_{oM,i_M}\right). \end{aligned} \tag{51}$$

References

[1] F.-T. Chien, C.-H. Hwang, and C.-C. Kuo, "Analysis of asynchronous long-code multicarrier CDMA systems with correlated fading," *IEEE Trans. Commun.*, vol. 53, no. 4, pp. 666–676, Apr. 2005.

[2] J. Namgoong, T. Wong, and J. Lehnert, "Subspace multiuser detection for multicarrier DS-CDMA," *IEEE Trans. Commun.*, vol. 48, no. 11, pp. 1897–1908, Nov. 2000.

[3] S. Hara and R. Prasad, "Overview of multicarrier CDMA," *IEEE Commun. Mag.*, vol. 35, no. 12, pp. 126–133, Dec. 1997.

[4] D. K. Kim and S.-H. Hwang, "Capacity analysis of an uplink synchronized multicarrier DS-CDMA system," *IEEE Commun. Lett.*, vol. 6, no. 3, pp. 99–101, Mar. 2002.

[5] L.-L. Yang and L. Hanzo, "Serial acquisition performance of single-carrier and multicarrier DS-CDMA over Nakagami-m fading channels," *IEEE Trans. Wireless Commun.*, vol. 1, no. 4, pp. 692–702, Apr. 2002.

[6] L.-L. Yang and L. Hanzo, "Performance of generalized multicarrier DS-CDMA over Nakagami-m fading channels," *IEEE Trans. Commun.*, vol. 50, no. 6, pp. 956–966, Jun. 2002.

[7] L.-L. Yang and L. Hanzo, "Multicarrier DS-CDMA: A multiple access scheme for ubiquitous broadband wireless communications," *IEEE Commun. Mag.*, vol. 41, no. 10, pp. 116–124, Oct. 2003.

[8] L.-L. Yang, W. Hua, and L. Hanzo, "A multicarrier DS-CDMA system using both time-domain and frequency-domain spreading," in *Proc. IEEE Veh. Technol. Conf.*, Orlando, FL, Oct. 2003, vol. 4, pp. 2426–2430.

[9] C. W. You and D. S. Hong, "Multicarrier CDMA systems using time-domain and frequency-domain spreading codes," *IEEE Trans. Commun.*, vol. 51, no. 1, pp. 17–21, Jan. 2003.

[10] C.-M. Yang, P.-H. Lin, G.-C. Yang, and W. C. Kwong, "2D orthogonal spreading codes for multicarrier DS-CDMA systems," in *Proc. IEEE Int. Conf. Commun.*, Anchorage, AK, May 2003, vol. 5, pp. 3277–3281.

[11] P.-W. Fu and K.-C. Chen, "Multi-rate MC-DS-CDMA with multiuser detections for wireless multimedia communications," in *Proc. IEEE Veh. Technol. Conf.*, Birmingham, AL, May 2002, vol. 3, pp. 1536–1540.

[12] L.-C. Wang and C.-W. Chang, "On the performance of multicarrier DS-CDMA with imperfect power control and variable spreading factors," *IEEE J. Sel. Areas Commun.*, vol. 24, no. 6, pp. 1154–1166, Jun. 2006.

[13] S. P. Chang and K. B. Lee, "Transmit power allocation for BER performance improvement in multicarrier systems," *IEEE Trans. Commun.*, vol. 52, no. 52, pp. 1658–1663, Oct. 2004.

[14] H. Long and Y. H. Chew, "An adaptive subcarrier allocation scheme for MC-DS-CDMA systems in the presence of multiple access interference," in *Proc. IEEE Int. Conf. Commun.*, Paris, France, Jun. 2004, vol. 5, pp. 2894–2898.

[15] H. Wei, L.-L. Yang, and L. Hanzo, "Time- and frequency-domain spreading assisted MC-DS-CDMA using interference rejection spreading codes for quasi-synchronous communications," in *Proc. IEEE Veh. Technol. Conf.*, Milan, Italy, Sep. 2004, vol. 1, pp. 389–393.

[16] H. Wei, L.-L. Yang, and L. Hanzo, "Interference-free broadband single and multicarrier DS-CDMA," *IEEE Commun. Mag.*, vol. 43, no. 2, pp. 68–73, Feb. 2005.

[17] S. Sureshkumar, E. Shwedyk, and H. H. Nguyen, "MAI-minimized signature waveforms for MC-DS-CDMA systems," in *Proc. IEEE Veh. Technol. Conf.*, Stockholm, Sweden, Jun. 2005, vol. 1, pp. 305–309.

[18] M. Amadei, U. Manzoli, and M. Merani, "On the assignment of Walsh and quasi-orthogonal codes in a multicarrier DS-CDMA system with multiple classes of users," in *Proc. IEEE Global Telecommun. Conf.*, Taipei, Taiwan, R.O.C., Nov. 2002, vol. 1, pp. 841–845.

[19] U. Manzoli and M. Merani, "Multicarrier DS-CDMA performance with different assignment strategies of quasi-orthogonal codes," in *Proc. IEEE Int. Symp. Pers., Indoor Mobile Radio Commun.*, Lisbon, Portugal, Sep. 2002, vol. 4, pp. 1477–1481.

[20] L.-C. Wang, C.-W. Chang, and H. Huang, "An interference avoidance code assignment strategy for downlink multi-rate MCDS-CDMA with TF-domain spreading," *IEEE Trans. Wireless Commun.*, vol. 6, no. 7, pp. 2508–2518, Jul. 2007.

[21] K. S. Lim and J. H. Lee, "Performance of multirate transmission schemes for a multicarrier DS/CDMA system," in *Proc. IEEE Veh. Technol. Conf.*, Atlantic City, NJ, Oct. 2001, vol. 2, pp. 767–771.

[22] T. Ottosson and A. Svensson, "On schemes for multirate support in DS-CDMA systems," *Wirel. Pers. Commun.*, vol. 6, no. 3, pp. 265–287, Mar. 1998.

[23] Y.-C. Tseng, C.-M. Chao, and L.-C. Wang, "Reducing internal and external fragmentations of OVSF codes in WCDMA systems with multiple codes," *IEEE Trans. Wireless Commun.*, vol. 4, no. 4, pp. 1516–1526, Jul. 2005.

[24] Y. Zhu and E. Gunawan, "Performance of MC-CDMA system using controlled MRC with power control in Rayleigh fading channel," *Electron. Lett.*, vol. 36, no. 8, pp. 752–753, Apr. 2000.

[25] M. Abramowitz and I. A. Stegun, *Handbook of Mathematical Functions With Formulas, Graphs, and Mathematical Tables*, ser. U.S. Dept. Nat. Bur. Stand. Applied Mathematics Series 55. New York: Dover, 1964.

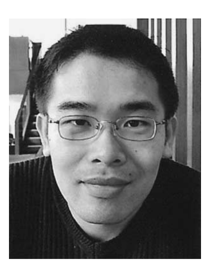

Chih-Wen Chang (S'02–M'06) received the B.S. and M.S. degrees in electrical engineering from National Sun Yat-Sen University, Kaohsiung, Taiwan, R.O.C., in 1998 and 2000, respectively, and the Minor M.S. degree in applied mathematics and the Ph.D. degree in communication engineering from National Chiao Tung University, Hsinchu, Taiwan, in 2005 and 2006, respectively.

Since August 2006, he has been an Assistant Professor with the Institute of Computer and Communication Engineering, National Cheng Kung University, Tainan, Taiwan. His current research interests include cognitive radio, optimization, and cross-layer design in wireless communication systems.

Dr. Chang was awarded the IEEE Student Travel Grant for the 2006 International Conference on Communications and membership into the Phi Tau Phi Scholastic Honor Society in 2006.

Li-Chun Wang (S'92–M'96–SM'06) received the B.S. degree from National Chiao Tung University (NCTU), Hsinchu, Taiwan, R.O.C., in 1986, the M.S. degree from National Taiwan University, Taipei, Taiwan, in 1988, and the M.Sci. and Ph.D. degrees from the Georgia Institute of Technology, Atlanta, in 1995 and 1996, respectively, all in electrical engineering.

From 1990 to 1992, he was with the Telecommunications Laboratories, Ministry of Transportations and Communications, Taiwan (currently the Telecom Labs, Chunghwa Telecom Company). In 1995, he was affiliated with Bell Northern Research, Northern Telecom, Inc., Richardson, TX. From 1996 to 2000, he was a Senior Technical Staff Member with the Wireless Communications Research Department, AT&T Laboratories. Since August 2000, he has been an Associate Professor with the Department of Communication Engineering, NCTU, where he became a Full Professor in August 2005. His current research interests are in the areas of adaptive/cognitive wireless networks, radio network resource management, cross-layer optimization, and cooperative wireless communication networks. He is the holder of three U.S. patents. He has published over 30 journals and 70 international conference papers.

Dr. Wang has served as an Associate Editor for the IEEE TRANSACTIONS ON WIRELESS COMMUNICATIONS from 2001 to 2005 and the Guest Editor of the special issue on "*Mobile computing and networking*" for the IEEE JOURNAL ON SELECTED AREAS IN COMMUNICATIONS in 2005 and the special issue on "*Radio resource management and protocol engineering in future IEEE broadband networks*" for the *IEEE Wireless Communications Magazine* in 2006. He is a corecipient (with G. L. Stuber and C.-T. Lea) of the 1997 Jack Neubauer Best Paper Award from the IEEE Vehicular Technology Society.